PERGAMON

Vision Research 39 (1999) 1641–1656

Vision Research

Temporal sensitivity of human luminance pattern mechanisms determined by masking with temporally modulated stimuli

Geoffrey M. Boynton [a,*], John M. Foley [b]

[a] *SNL-B, The Salk Institute for Biological Studies, PO Box 85800, San Diego, CA 92186-5800, USA*
[b] *Department of Psychology, University of California, Santa Barbara, CA, USA*

Received 12 May 1997; received in revised form 8 April 1998

Abstract

Target contrast thresholds were measured using vertical spatial Gabor targets in the presence of full field maskers of the same spatial frequency and orientation. In the first experiment both target and masker were 2 cpd. The target was modulated at a frequency of 1 or 10 Hz and the maskers varied in temporal frequency from 1 to 30 Hz and in contrast from 0.03 to 0.50. In the second experiment both target and masker had a spatial frequency of 1, 5 or 8 cpd. The target was modulated at 7.5 Hz and the same set of maskers was used as in the first experiment. The results are not consistent with a widely used model that is based on mechanisms in which excitation is summed linearly and the sum is transformed by an S-shaped nonlinear excitation-response function. A new model of human pattern vision mechanisms, which has excitatory and divisive inhibitory inputs, describes the results well. Parameters from the best fit of the new model to the results of the first experiment show that the 1 Hz and 10 Hz targets were detected by mechanisms with temporal low-pass and band-pass excitatory sensitivity, respectively. Fits to the second experiment suggest that at 1 cpd, the excitatory tuning of the detecting mechanism is band-pass. At 5 and 8 cpd, the mechanisms are excited by a broad range of temporal frequencies. Mechanism sensitivity to divisive inhibition depends on temporal frequency in the same general way as sensitivity to excitation. Mechanisms are more broadly tuned to divisive inhibition than to excitation, except when the target temporal frequency is high.

Keywords: Masking; Spatio-temporal frequency; Inhibition; Contrast

1. Introduction

Current theories of human pattern vision hold that the initial stages of visual processing involve an array of mechanisms, each responsible for detection within a subset of the stimulus domain. The first evidence was derived from experiments on the detection of spatial patterns that suggested the existence of mechanisms differentially tuned to spatial frequency (Campbell & Robson, 1967). The idea that these mechanisms can also be characterized by their temporal properties soon followed. Early experiments showed that the shape of the temporal contrast sensitivity function (TCSF) varies with spatial frequency (Robson, 1966; van Nes, Koenderink, Nas & Bouman, 1967; Kelly, 1972; Koenderink & van Doorn, 1979). At low spatial frequencies, the TCSF has a band-pass temporal characteristic, while low-pass characteristics are found at high spatial frequencies. As a consequence, if there are mechanisms with different spatial frequency tuning they must also differ in temporal tuning.

A variety of additional psychophysical techniques have been used to investigate the temporal properties of individual pattern vision mechanisms. These include phenomenological threshold sensation experiments (Keesey, 1972; Kulikowski & Tolhurst, 1973; King-Smith & Kulikowski, 1975; Green, 1981), pattern adaptation to gratings (Green, 1981), discrimination at threshold (Watson & Robson, 1981; Thompson, 1983; Hess & Plant, 1985), discrimination above threshold (Mandler, 1984; Mandler & Makous, 1984), metameric matching of temporal frequencies (Richards, 1979), subthreshold summation (Tolhurst, 1975; Breitmeyer & Ganz, 1977), motion direction discrimination (Anderson & Burr, 1985), reaction times to the onset of

* Corresponding author. Tel.: +1 619 4534100 x1545; fax: +1 619 546 8526; e-mail: boynton@salk.edu.

0042-6989/99/$ - see front matter
PII: S0042-6989(98)00199-0

gratings (Breitmeyer, 1975; Tartaglione, Goff, & Benton, 1975; Harwerth & Levi, 1978) and measures of response integration time (Breitmeyer & Ganz, 1977; Legge, 1978). This literature was reviewed by Watson (1986). These experiments show that there are only a few temporal mechanisms operating at a given spatial frequency. At low spatial frequencies, inferred mechanisms generally have band-pass characteristics and low-pass temporal tuning is found at high spatial frequencies.

The paradigm used in this study is simultaneous masking. Simultaneous masking occurs when one transient stimulus (the masker) reduces the detectability of another stimulus (the target). A common model of the pattern vision mechanism associated with masking experiments assumes a spatiotemporal linear filter followed by an invariant S-shaped contrast response function (Legge & Foley, 1980; Wilson, McFarlane & Phillips, 1983). Masking is predicted with the Fechnerian notion that the target, at threshold, produces a constant increment in the mechanism's response above the response to the masker alone. Masking occurs when the masker increases the response of the mechanism to where the slope of the response function begins to decrease, requiring a higher target contrast to produce the increment in response required for detection. We call this the nonlinear excitation model (or NE model) of pattern masking.

Two lines of evidence for multiple mechanisms differing in temporal sensitivity come from the application of the NE model to masking results. First, the shape of the function that relates target contrast at threshold to masker contrast, or TvC function, varies with spatial and temporal frequency of the target. When target and masker have low spatial and high temporal frequencies, the rising portion of the TvC function is steeper than for high spatial and low temporal frequencies (Burbeck & Kelly, 1980; Pantle, 1983; Lehky, 1985; Hess & Snowden, 1992). According to the NE model, the contrast response function for low spatial/high temporal frequency mechanisms shows greater response compression than for high spatial/low temporal frequency mechanisms. Since the shape of the contrast response function is constant for a single mechanism, these results suggest that at least two classes of mechanisms exist.

The second line of evidence comes from masking functions, which relate target threshold to masker temporal frequency. Masking functions are obtained by fixing the temporal frequency of the target and varying the temporal frequency of the masker at a fixed masker contrast. According to the NE model, masking functions are sufficient to determine the sensitivity of detecting mechanisms (up to a scale factor) in a manner analogous to Stiles (1949) field sensitivity measurements of chromatic mechanisms. Lehky (1985) and Hess and Snowden (1992) measured masking functions and estimated the temporal sensitivity of the detecting mechanism by fitting variations of the NE model to psychophysical results.

Recent work has cast doubt on whether the NE model, whether used explicitly or implicitly, is correct (Foley, 1994; Foley & Boynton, 1994). In the present study we test the NE model in the temporal domain by measuring the entire TvC function for each of several masker temporal frequencies. The experiments in this paper concern the detectability of Gabor patterns that are simultaneously masked by gratings of the same spatial frequency and orientation. Both masker and target are temporally modulated in counterphase. By using five target stimuli we test the model for different regions of the spatio-temporal domain. We show that the NE model is inconsistent with our results for all five targets. As an alternative, we describe a new model of the human pattern vision mechanism (Foley, 1994; Foley & Boynton, 1994) in which each mechanism has a divisive inhibitory input in addition to a linear excitatory input. We call this the divisive inhibition model (or DI model) in this paper. We show that the new model fits the data well and provides parameter values that characterize the temporal properties of pattern vision mechanisms. Since the past masking experiments have been interpreted using the NE model of masking, the studies reviewed above are re-evaluated in light of the new model.

The models that we consider are functional models in the sense that they attempt to describe the relation between the stimuli and performance. The models assume pattern vision mechanisms that resemble cortical simple cells in some respects, but we do not identify them with cells; they are defined solely by their mathematical properties. Unlike other models (Teo & Heeger, 1994; Watson & Solomon, 1997), our models do not assume specific spatial and temporal sensitivity functions for the mechanisms. Instead, they allow mechanism sensitivities to be estimated from experimental data. If sensitivities are estimated for a set of sinewave gratings that differ along some dimension (e.g. spatial or temporal frequency), we can use these to estimate mechanism sensitivity along the corresponding dimension (space or time). Thus we assume only the most fundamental properties of the mechanisms and allow other properties, such as sensitivity, to be estimated on the basis of experimental data. The models are evaluated both by their qualitative predictions and their ability to fit data. In spite of their flexibility, if functional models of this kind can be found that will fit a large body of data well, they will provide a concise way to summarize families of TvC functions and thus show the constraints that any structural model of these phenomena must satisfy.

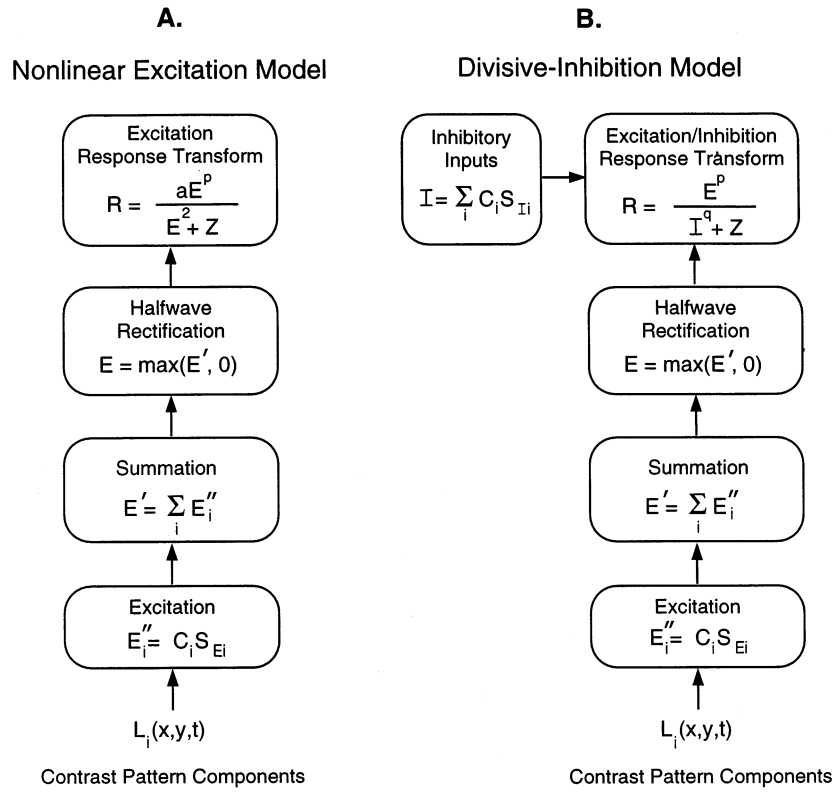

Fig. 1. The NE model (A) and the DI model (B) of human luminance pattern vision mechanisms. In addition to linear summation of excitation over a receptive field the DI model assumes a mechanism that receives a broadband inhibitory input which is independent of excitation.

The three models that were tested in this study are described in the following section.

2. Models

2.1. Single-mechanism nonlinear excitation model (NE_1)

Fig. 1A illustrates the single-mechanism nonlinear excitation (NE_1) model of human pattern vision mechanisms. The input stimulus, whether masker or target plus masker is comprised of pattern components, which in our case are sinewave gratings and Gabor patterns. The contrast of these patterns is defined as (peak luminance − background luminance)/background luminance. This is equivalent to Michelson contrast for sinewave components. Since our patterns vary in time, the response of the detecting mechanisms very likely varies in time. However, we assume that the detection of our target patterns depends on the response of the detecting mechanism at one moment in time, which in turn depends on the input to the mechanism at that moment.

The excitation of the mechanism produced by any pattern component is given by:

$$E''_i = C_i S_{Ei} \tag{1}$$

Where C_i is the contrast of that component and S_{Ei} is the excitatory sensitivity of the mechanism to that component.

Net excitation is the sum of excitation across all pattern components.

$$E' = \sum_i E''_i \tag{2}$$

Net excitation is halfwave rectified:

$$E = \max(E', 0) \tag{3}$$

and fed into an S-shaped static nonlinearity $R(E)$:

$$R(E) = \frac{E^p}{E^2 + Z} \tag{4}$$

The parameters p and Z characterize the mechanism, and are constant within a family of TvC functions.

This model was not adequately tested until recently. One testable implication is that if a single mechanism detects a target, any masker that excites the mechanism can only shift the TvC function along the masker contrast axis by a multiplicative constant (Foley, 1994). However, Ross and Speed (1991) and Foley (1994) showed that this horizontal translation rule fails for maskers that are very different from the target in either orientation or spatial frequency.

2.2. Two-mechanism nonlinear excitation model (NE_2)

One possible way to reconcile the violation of the horizontal translation rule is to assume that more than one mechanism is involved in the detection of the target. The NE model can easily be extended to assume multiple independent mechanisms. If there are two mechanisms, the response of each mechanism is:

$$R_1(E) = \frac{E_1^p}{E_1^2 + Z_1}$$

$$R_2(E) = \frac{E_2^p}{E_2^2 + Z_2}$$

The combined response across the two mechanisms is:

$$R(E) = (R_1^n + R_2^n)^{1/n} \quad (5)$$

Where $n \geq 2$. The NE_2 model makes similar predictions to the NE_1 model, except that the rising portion of the predicted TvC functions may show scallops at the target contrast threshold where the second mechanism takes over the role of detecting the target.

The one and two mechanism nonlinear excitation models were recently shown to be unable to predict masking results in which the relative orientation of the masker to target is varied (Foley, 1994; Foley & Boynton, 1994).

2.3. Divisive inhibition model (DI)

This failure led to a new model of human pattern vision mechanisms (Foley, 1994; Foley & Boynton, 1994). This model was inspired by models of neurophysiology of cells in visual cortex (Albrecht & Geisler, 1991; Heeger, 1992). According to this divisive inhibition (DI) model, pattern masking is a consequence of divisive suppression. The model describes masking results for maskers that vary in orientation, contrast and spatial phase as well as for combinations of two maskers. Fits of the model to these results show that the sensitivity to excitatory inputs is more narrowly tuned than sensitivity to divisive inhibitory inputs.

Foley (1994) describes two versions of the DI model. The version described in the present study is his model 2 and is illustrated in Fig. 1B. In this model excitation is computed as in Eqs. (1)–(3). The inhibition, produced by the components of the stimulus, is summed linearly. For temporally modulated stimuli, inhibition may vary in time. However, as with excitation we assume that the threshold depends on the inhibition at one moment in time. The inhibition is given by:

$$I = \sum_i C_i S_{Ii} \quad (6)$$

The mechanism response is given by:

$$R(E, I) = \frac{E^p}{I^q + Z} \quad (7)$$

A comparison of Eq. (4) and Eq. (7) shows that the divisive inhibition model is formally a more general version of the nonlinear excitation model. If $I = E$ and $q = 2$, the two models are mathematically identical. Since I and E are not always equal, it makes sense to interpret them as a separate inputs to the mechanism.

2.4. Predicting masking results from models

The models described above can predict masking results through the assumption that a target is detectable only when the response of the mechanism to the target and masker combined exceeds the response to the masker alone by a fixed increment. For the DI model, let E_m and I_m be the excitatory and inhibitory inputs to the mechanism produced by the masker, and E_{mt} and I_{mt} be the excitatory and inhibitory inputs produced by the target and masker combined. Then the target is at threshold if:

$$R(E_{mt}, I_{mt}) - R(E_m, I_m) = 1 \quad (8)$$

It is of interest to look at the model's predictions of the TvC function for different parameter values. Consider the case where $S_{Em} = 0$, and hence $E_m = 0$ and $R(E_m, I_m) = 0$. The target is therefore at threshold when: $R(E_t, I_{mt}) = 1$. Where E_t is the excitatory response to the target alone. When the masker and target are presented together, the denominator of the response transform increases monotonically with masker contrast while the numerator depends only on target contrast. Thus the contrast of the target must increase with masker contrast to keep the response of the target plus masker at threshold. This is pure divisive inhibitory masking. Fig. 2 shows predicted TvC functions using typical parameter values. Note that for pure divisive inhibitory masking, the TvC function rises monotonically without a dip (facilitation).

Fig. 2 also shows a TvC function for $S_{Em} > 0$, where the DI model's predictions are much like that of the nonlinear excitation model. The familiar dipper-shaped TvC function is predicted.

The DI model predicts that if S_{Em} and S_{Im} are scaled by the same constant, then the TvC function shifts horizontally on log-log coordinates. Scaling S_{Et} and S_{It} together shifts the TvC function vertically on log–log coordinates, much like the nonlinear excitation model.

However, unlike the NE models, an increase of S_{Em} with respect to S_{Im} enhances the predicted facilitation and therefore changes the shape of TvC function.

Our goal in this study is to test these three models of human pattern vision mechanisms. The best fitting model will be used to estimate mechanism parameters, including sensitivities.

3. Methods

3.1. Equipment

Stimuli were generated using a computer graphics system that consisted of an AST 386/20 computer, a Truevision ATVISTA graphics board with 2 MB video memory, a contrast mixer and attenuator circuit, and two video monitors operating at a 60 Hz frame rate. Truevision Stage graphics software was used for image generation and control. The maskers and targets were generated on two different monitors and were combined by a beam splitter. Images of the fixation field, the masker field and the target field were computed and stored on the graphics board. Each of these images was 512×400 pixels and the intensity at each point was specified by an 8-bit number. The methods of contrast control are described by Watson, Nielson, Poirson, Fitzhugh, Bilson, Nguyen and Nguyen (1986) and were adapted to the masking paradigm and to our system. The contrasts of the masker and target were controlled by the green and red channels of the graphics system, respectively. An external analog circuit attenuated one or both of these signals. A blue channel signal was added to these to maintain constant mean luminance. The combined signal was then directed to the green input line of a monitor so that all of the stimuli were monochrome green. The lookup tables had the dual role of determining contrast and correcting for the nonlinear relation between voltage and screen intensity. As a consequence, the number of possible intensities in each pattern component was approximately 180. Two ranges of contrast were made possible by the attenuator circuit so that low contrast patterns could be presented without loss of wave-form definition.

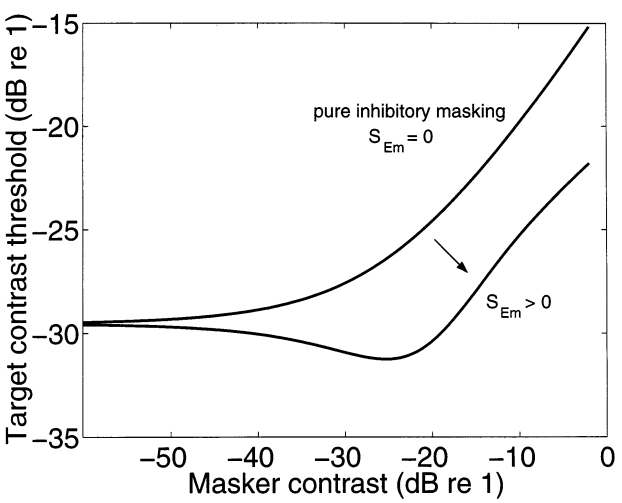

Fig. 2. DI model's prediction of the TvC function with and without excitatory sensitivity to the masker. Parameter values are: $S_{Em} = 0$ and 10, $S_{Im} = 10$, $S_{Et} = 50$, $S_{It} = 30$, $P = 2.4$, $q = 2.0$, $Z = 1.0$. Target is detectable when the response to the masker plus target exceeds the response to the masker alone by 1.0.

3.2. Stimuli

Viewing distance was 162 cm and the visual angle subtended by the stimulus field was 7° horizontal × 5° vertical. The mean luminance was 33 cd/m^2. The fixation field was uniform except for a small dark fixation point at the center. The surround was dark.

Spatially, all maskers were vertical sinewave gratings that filled the entire field. Targets were Gaussian windowed vertical sinewave gratings (Gabor patterns) with center spatial frequencies equal to the spatial frequency of the masker. Maskers and targets were both in cosine phase with the fixation point. The Gaussian window of the target was centered on the fixation point and had an 1/e space constant of 1.875° in both vertical and horizontal directions except for the 5 cpd condition of Experiment 2 where the half-width was 0.375°. Spatially restricted targets were used so that they would stimulate a region of the retina that is relatively homogeneous with respect to spatial properties. Contrast for both patterns was defined as (peak luminance − background luminance)/background luminance. This is equivalent to Michelson contrast for the sinewave maskers. Contrast is measured in decibels (dB re 1) where 1 dB is one twentieth of a log unit.

Temporal profiles of a typical target and masker are shown in Fig. 3A. Temporally, all maskers were modulated in counterphase. Masker duration was 667 ms (40 frames) and modulation was in cosine phase with the center of the presentation interval. The limited frame rate (60 Hz) of the monitors means that the temporal profile is only approximately sinusoidal even at low temporal frequencies. At temporal frequencies above 15 Hz the masker temporal waveform was a square-wave. Targets were Gabor patterns in time modulated within a Gaussian window with an 1/e time constant of 105 ms (6.33 frames). Both the cosine phase of the carrier frequency and the Gaussian window of the Gabor target were centered in the masker's presentation interval. The target reached peak contrast 333 ms after the onset of the masker, a period long enough that the transience of the onset should not have influenced target detection. The short duration of the target produces a fairly broad band-width in temporal frequency spectrum. The amplitude spectrum of the three target stimuli used in this paper are shown Fig. 3B. We refer to targets by the temporal frequency of the cosine-wave that is modulated by the Gaussian envelope.

3.3. Procedure

A two position spatial forced-choice method was used to determine target contrast thresholds. On each trial the target was presented with equal probability either centered 0.8° directly above or below the fixation point. A tone was presented during the target interval.

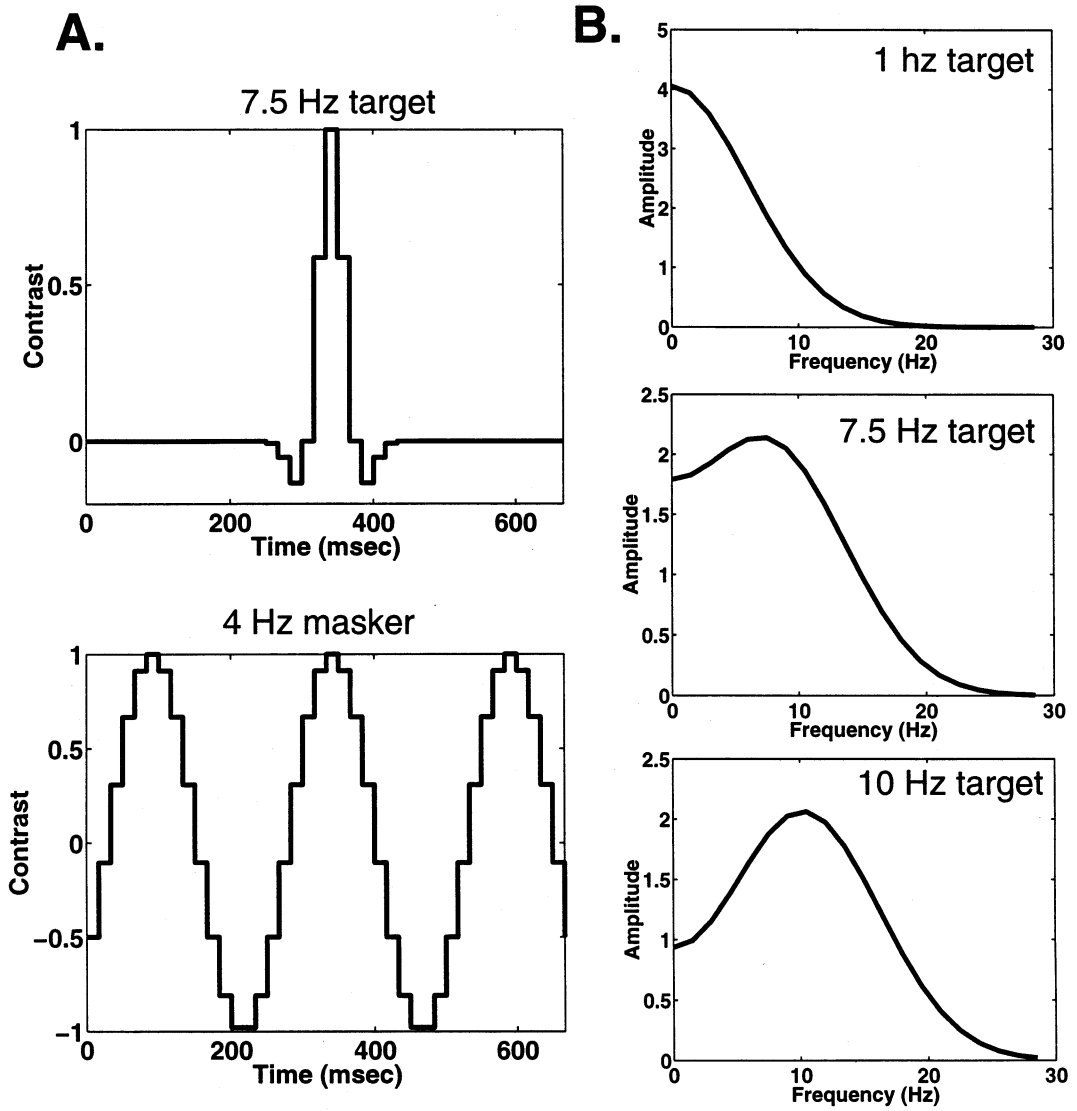

Fig. 3. (A) Temporal profiles of a target and masker. (B) Amplitude spectra of the three targets used in Experiments 1 and 2. Target contrasts are a Gabor functions in time with a 1/e time constant of 105 ms.

The observer responded by pushing a lever forward or back to indicate target 'above' or 'below'. The response was followed by a high or a low tone indicating correct or incorrect. The QUEST procedure (Watson & Pelli, 1983) was used to adjust the contrast so as to seek the contrast corresponding to a probability correct of 0.92. As pointed out by Watson and Pelli (1983), the 0.92 probability correct criterion minimizes the 'sweat factor' which, for the QUEST procedure, places the intensities during the staircase sequence at locations that are optimal for estimating the position of the psychometric function. The sequence was terminated after 40 trials, or 50 trials if there were no errors on the last 20 trials. Each condition was repeated three or four times and conditions were presented in a random order blocked by masker temporal frequency.

3.4. Subjects

One of the authors, GMB, served as a subject. A second subject, JYS, was a 20 year old female undergraduate student at the University of California at Santa Barbara. Both subjects had resolution acuity of 20/20 without correction and were highly practiced psychophysical observers. JYS was naive in regard to the purpose of these experiments.

3.5. Experiment 1

3.5.1. Target and masker spatial frequency 2 cpd; two target temporal frequencies of 1 and 10 Hz

Table 1 summarizes the design of the experiment. All stimuli had a spatial frequency of 2 cpd. Both low and

Table 1
Experimental variables, details of theoretical analysis, and parameter values of the best fitting DI model

	Spatial		Temporal	
Experimental variables				
Masker	full-field 7 × 5°; 2 cpd		667 ms rect.; 1, 5, 10, 20, 30 Hz	
Target	Gabor 1.875°; 2 cpd		Gabor 105 ms; 1, 10 Hz	
	GMB		JYS	
Target frequency (Hz)	1	10	1	10
Theoretical analysis				
No. of data points	60	59	60	58
Measurements per point	4	4	3	3
Mean standard error (dB)	0.83	0.73	0.71	0.84
Free parameters				
NE_1	8	8	8	8
NE_2	14	14	14	14
DI	14	14	14	14
SSE (dB^2)				
NE_1	149.12	201.71	6.16	132.36
NE_2	60.74	62.34	54.13	91.88
DI	52.85	62.4	48.67	66.22
MSE (dB^2/data point)				
NE_1	2.49	3.42	1.60	2.28
NE_2	1.01	1.06	0.90	1.58
DI	0.88	1.06	0.81	1.14
F test (DI over NE)	$P<0.0001$	$P<0.0001$	$P<0.0001$	$P<0.0001$
DI parameters				
S_{Et}	66.46	93.00	46.13	61.55
S_{It}	14.96	50.98	33.24	39.63
p	2.52	1.39	2.36	1.64
q	2.13	1.08	1.97	1.24
Z (fixed)	1.00	1.00	1.00	1.00

Mean luminance 33 cpd/m^2.

high temporal frequency targets (1 and 10 Hz) were detected in the presence of a masker modulating at 1, 5, 10, 20 or 30 Hz. These low and high target temporal frequencies were chosen so that if there are mechanisms tuned to different ranges of temporal frequency, they are likely to be detected by different mechanisms. A TvC function was measured for each masker and target frequency combination by using several masker contrasts ranging from -50 to -6 dB re 1, as well as a zero contrast masker. Each condition was repeated three or four times. Thus, for each of the two targets, a set of five TvC functions was measured. A set of TvC functions that share a common target configuration will be called a family of TvC functions. A diagram showing the stimulus conditions in spatio-temporal space is shown in Fig. 4A.

3.6. Experiment 2

3.6.1. Target of 7.5 Hz with spatial frequencies of 1,5 and 8 cpd

Fig. 4B illustrates the stimulus conditions in Experiment 2. The experimental design is shown in Table 2. The target temporal frequency was always 7.5 Hz and the spatial frequency of target and masker were varied together. Since the temporal contrast sensitivity function is band-pass at low spatial frequencies and low-pass at high spatial frequencies (Robson, 1966; Kelly, 1972), manipulating the spatial frequency of the target and masker is a second way to favor particular classes of detecting mechanism (Breitmeyer & Ganz, 1977). Each target was detected in the presence of a masker modulating at 1, 4, 7.5, 15 or 30 Hz. Masker and target spatial frequencies were either 1 or 8 cpd for JYS and 1, 5 or 8 cpd for GMB. One family of TvC functions was measured for each spatial frequency.

4. Results

4.1. Experiment 1

Figs. 5 and 6 show the results for subjects GMB and JYS, respectively. Contrast is measured in decibels (dB re 1) where 1 dB is one twentieth of a log unit. The results for the 1 and 10 Hz targets are shown above (A) and below (B), respectively. Solid lines show the best fit of the DI model to the data and are discussed in the next section.

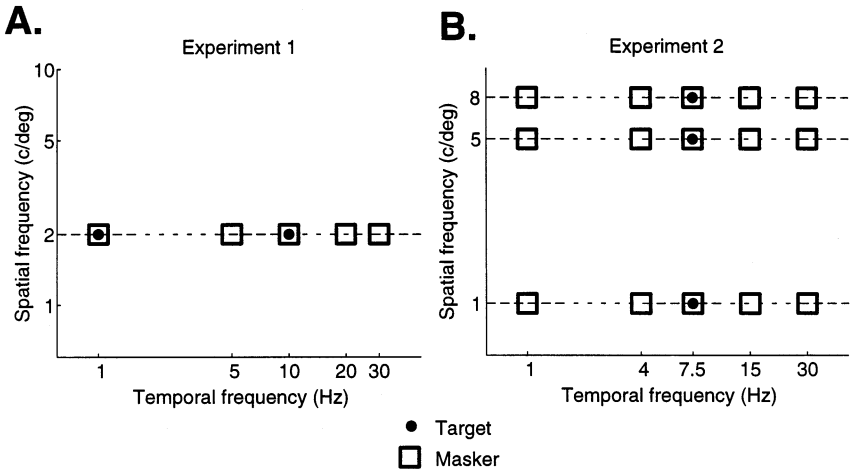

Fig. 4. Experimental conditions in Experiment 1 (A) and Experiment 2 (B). The spatial and temporal frequencies of maskers and targets are denoted by open squares and filled circles, respectively. Each target was detected in the presence of all five maskers of the same spatial frequency. An entire TvC function was measured for each masker and target combination.

The thresholds shown are means of three (JYS) or four (GMB) measurements. The standard errors of the mean were roughly equal for all masker temporal frequencies and increased by a factor of about 1.2 from low to high masker contrasts. Mean standard errors are shown in Table 1.

There is remarkable similarity between the two subjects. The shape of the TvC functions varies with masker temporal frequency in two ways. First, facilitation is greatest when masker and target frequencies are the same for both the 1 and 10 Hz targets. Facilitation decreases as the difference between target and masker frequency increases. Second, the slopes of the rising portion of the TvC functions vary within a family. Table 3 shows the slopes of the best fitting lines (method of least-squares) through the rising portions of each TvC function. Data included in the slope analysis were subjectively defined; points from the highest masker contrasts were chosen from a region where a straight line appeared to fit the data well. For the 1 Hz target, slopes are steepest at the intermediate masking frequency of 10 Hz. For the 10 Hz target, slopes generally increase with masker frequency. The change in slope violates the horizontal displacement rule and is inconsistent with the NE_1 model. The decrease in facilitation is inconsistent with models NE_1 and NE_2.

Note also that maximum masking does not occur at the target frequency. The 1 Hz target is masked maximally by a 10 Hz masker and the 10 Hz target is masked maximally by a 20 Hz masker. Masking is greater at the masker frequencies above and below the 10 Hz target frequency than at the 10 Hz masker frequency.

Phenomenological reports from both subjects indicate that the percept does not vary systematically within a family of TvC functions. For all masker frequencies, the 1 Hz target was described as an oriented pattern that gradually appeared and then disappeared. The 10 Hz target produced a flickering or flashing percept in the presence of all masker temporal frequencies. The spatial configuration of the 10 Hz target was described as 'blob-like'. Interestingly, these reports are similar to the phenomenological 'flicker' and 'pattern' criteria used by Kulikowski and Tolhurst in their investigations of independent temporal channels (Kulikowski & Tolhurst, 1973).

4.2. Experiment 2

Figs. 7 and 8 show the results of Experiment 2 for subjects GMB and JYS, respectively. Solid lines show the best fit of the DI model to the data. As in Experiment 1, the standard errors of the mean were roughly equal for all masker temporal frequencies and increased with masker contrast by a factor of about 1.3. Mean standard errors are shown in Table 2.

There is good agreement between the experimental results of the two subjects. As in Experiment 1, the results are inconsistent with the horizontal shift rule predicted by the NE model. Both the slopes of the rising portions of each TvC function and the amount of facilitation vary within a family of TvC functions. Slopes of the regression line through the rising portion of TvC functions are shown in Table 4. Slopes generally increase with the temporal frequency of the masker for all spatial frequencies, much like the slopes for the 10 Hz target in Experiment 1, but there is very little change in slope with spatial frequency. Facilitation is maximal when the masker frequency equals the target frequency of 7.5 Hz. Subjects reported that the 7.5 Hz target was described to 'flicker' or 'flash' at all spatial frequencies and appeared 'blob-like' in form.

Table 2
Experimental variables, details of theoretical analysis, and parameter values of the best fitting DI model

Experimental variables	Spatial			Temporal	
Masker	full-field 7×5°; 1, 5, 8 cpd			667 ms; rect 1, 4, 7.5, 15, 30 Hz	
Target	Gabor 1.875°; 1, 5, 8 cpd			Gabor 105 ms; 7.5 Hz	
Theoretical analysis	**GMB**			**JYS**	
Target frequency (cpd)	1	5	8	1	8
No. of data points	68	63	60	66	58
Measurements per point	4	48	4	3	3
Mean standard error (dB)	0.79	0.75	0.81	1.35	0.84
Free parameters					
NE_1	8	8	8	8	8
NE_2	14	14	14	14	14
DI	14	14	14	14	14
SSE (dB^2)					
NE_1	222.99	63.58	82.31	257.4	218.24
NE_2	127.42	42.39	64.20	213.38	166.61
DI	66.95	20.14	57.52	164.03	109.74
MSE (dB^2/data point)					
NE_1	3.28	1.01	1.37	3.90	3.67
NE_2	1.87	0.67	1.07	3.23	2.87
DI	0.98	0.32	0.96	1.90	1.89
F test (DI over NE)	$P<0.0001$	$P<0.0001$	$P<0.0001$	$P<0.0005$	$P<0.0001$
DI parameters					
S_{Et}	102.43	14.60	27.26	107.32	22.10
S_{It}	7.10	7.24	17.2	58.31	9.74
p	2.54	2.44	1.97	1.58	1.35
q	2.38	2.18	1.80	1.37	1.27
Z (fixed)	1.00	1.00	1.00	1.00	1.00

Again, maximum masking does not occur at the temporal frequency of 7.5 Hz. As in Experiment 1, masking is greater at the temporal frequencies below and above the target frequency.

5. Model fitting

Both the NE model (with one and two mechanisms) and the DI model were fitted to the data of Experiments 1 and 2. Both of the NE models make qualitative predictions that are inconsistent with the data. NE_1 predicts that any masker that excites the detecting mechanism will produce a TvC function which is a laterally shifted version of the others in our coordinates. The results clearly do not agree with that prediction. NE_2 predicts that the magnitude of facilitation will be the same for all maskers. The results do not agree with this prediction either. Legge and Foley, (1980) did show in the spatial domain that a NE model with multiple mechanisms can predict a decrease in facilitation as the difference between target and masker frequences increases. A similar analysis could apply in the temporal domain. However, this analysis assumes that there are multiple approximately equal peaks in the target waveform. That was not the case for our Gabor temporal waveforms. Nevertheless, we fitted all three models to our data.

The single-mechanism NE model (NE_1) requires four parameters for each TvC function. The two-mechanism NE model (NE_2) contains the same four parameters as NE_1 plus three more: additional excitatory sensitivities for the target and masker, and a nonlinear summation parameter, n. The parameter n was fixed to four, so the NE_2 model has six free parameters for a single TvC function. The DI model requires seven parameters for a single TvC function, but has only 6 d.f. (Appendix A). The parameter Z is therefore arbitrarily set to one. Table 5 is a description of the parameters for all three models.

The NE_1 model provides independent estimates of S_{Em} for each of the five masker frequencies in the

family. The remaining three parameters, S_{Et}, p, and Z are shared within the family, requiring a total of $5 + 3 = 8$ free parameters to predict a family of TvC functions (about 75 data points). The NE_2 model has six additional parameters (the five masker sensitivities and the one target sensitivity of the second mechanism). The DI model has independent estimates of S_{Em} and S_{Im} for each masker frequency in the family. The remaining four parameters, S_{Et}, S_{It}, p, and q are common to all TvC functions in the family, requiring a total of $2 \times 5 + 4 = 14$ free parameters to predict a family of TvC functions.

Fits of all three models to each family of TvC functions were obtained using an optimization procedure based on Powell's method (Press, Flannery, Teukolsky & Vetterling, 1988) of minimizing the sums of squared error (S.S.E.). For each family of TvC functions, 20 initial conditions were chosen by randomly perturbing the parameters from a set that provided a reasonable fit to the data. S.S.E. was then minimized using the optimization procedure for each of the 20 initial conditions. Of any set of 20 fits, parameter values of the best ten or so were approximately the same, indicating a global minimum of S.S.E. The parameter values from the best fit of these 20 optimizations were chosen as our estimate of the global minimum of S.S.E.

A statistical test of improvement in goodness of fit (Khuri & Cornell, 1987) was used to compare fits. This test takes into account the difference in the number of free parameters between one model and a more specific model that shares common, but fewer parameters. The test is in the form of the F statistic. The following is a description of the model fits for both experiments.

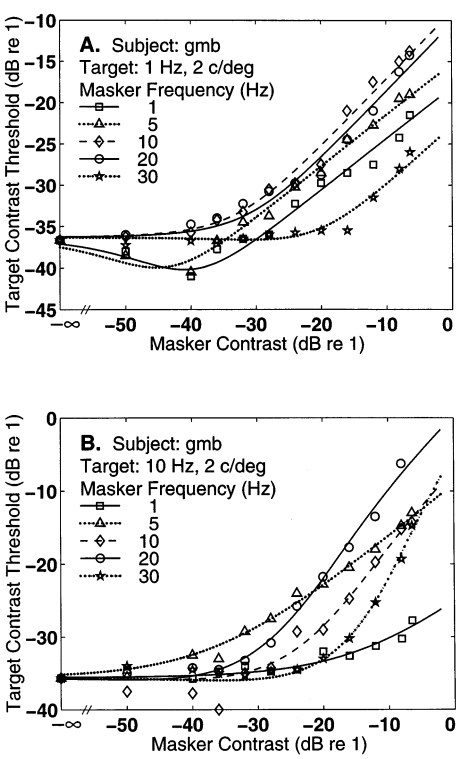

Fig. 5. Results of Experiment 1, subject GMB. Targets and maskers are 2 cpd. The results for the 1 and 10 Hz targets are shown above (A) and below (B), respectively.

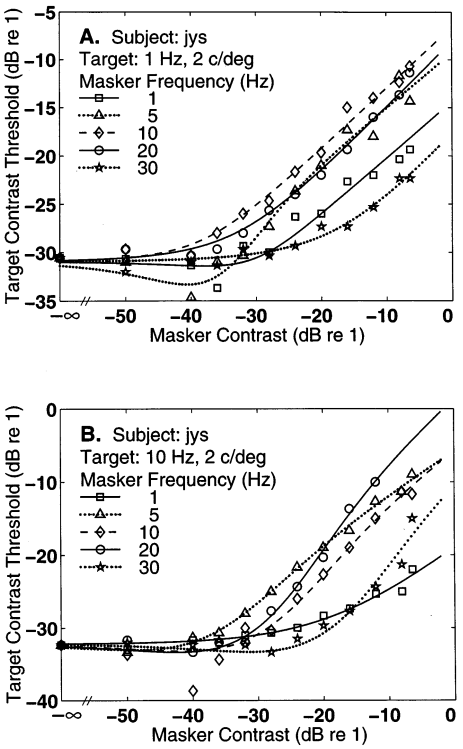

Fig. 6. Results of Experiment 1, subject JYS. Targets and maskers at 2 cpd. The results for the 1 and 10 Hz targets are shown above (A) and below (B), respectively.

5.1. Experiment 1

In each of the four families of TvC functions in Experiment 1, the DI model was significantly better in goodness-of-fit over the NE_1 model ($P < 0.001$). It is clear from Figs. 5 and 6 that the DI model fits the data well. The differing slopes are captured by the model. However, the model does not always capture facilitation well. The DI model also produced a better fit than the NE_2 model in three of the four cases (the fits were equally as good in the fourth), even though the number of parameters are the same.

Sums of squared errors (S.S.E.) for all three models are shown in Table 1. Mean standard error of the estimates and root mean squared error of the fit of the DI model are roughly similar, which indicates that the model is accounting for almost all of the effect except for random error. The parameter values from the best fits of the divisive inhibition model to the data, except for the sensitivities to the masker, are shown in Table 1.

Fig. 9 shows the excitatory and divisive inhibitory sensitivities of the detecting mechanism to maskers of different temporal frequencies. Functions for excitatory

Table 3
Slopes of regression line through the rising portion of TvC functions of Experiment 1

	GMB		JYS	
	1 Hz	10 Hz	1 Hz	10 Hz
1 Hz	0.52	0.30	0.46	0.40
5 Hz	0.62	0.60	0.67	0.72
10 Hz	0.81	0.93	0.60	0.89
20 Hz	0.92	1.16	0.61	1.15
30 Hz	0.74	1.55	0.43	0.97
Mean	0.722	0.908	0.554	0.826

sensitivity are low-pass for 1 Hz target (Fig. 9A,C) and band-pass for the 10 Hz target (Fig. 9B,D). The inhibitory sensitivity estimates show broader tuning than excitatory sensitivity. Recall that facilitation in the TvC functions (the dipper shape) is predicted by the divisive inhibition model when the excitatory sensitivity to the masker is high. The relatively narrow tuning of the excitatory sensitivity estimates in Fig. 9, therefore reflects the facilitation effects seen in the TvC functions when target and masker are similar in temporal frequency (Figs. 5 and 6).

5.2. Experiment 2

A statistical comparison of fits from the three models to the data of Experiment 2 shows that the DI model fits better than the NE_1 model for all three families of TvC functions ($P < 0.001$). It also fits better than the NE_2 model in all five cases. Table 2 shows the mean squared errors for all three models and all of the parameter values from the best fits of the DI model to the data except for the sensitivities to the masker, which are plotted in Fig. 10. As in Experiment 1, mean standard error of the estimates and root mean squared error of the fit of the DI model to the data are roughly similar. Although the fit is better than the NE models, the DI model fails to predict the facilitation found with subject JYS at both 1 and 8 cpd. The model appears not to be flexible enough to predict all aspects of these results.

Excitatory sensitivity estimates are band-pass at 1 and 5 cpd and low pass at 8 cpd. At 5 and 8 cpd,

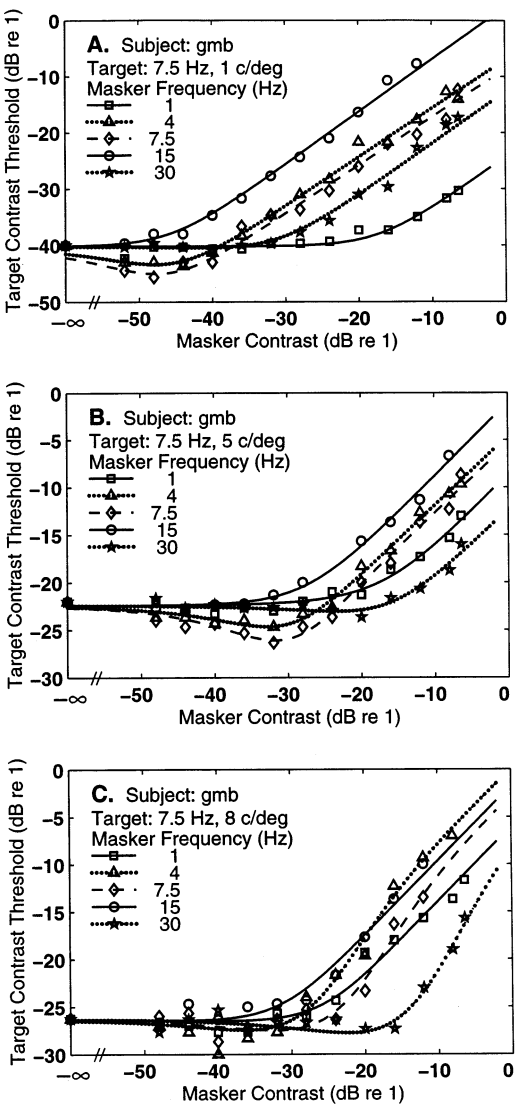

Fig. 7. Results of Experiment 2, subject GMB. All targets were 7.5 Hz. The three plots are for target and masker spatial frequencies of 1 (A), 5 (B) or 8 (C) cpd.

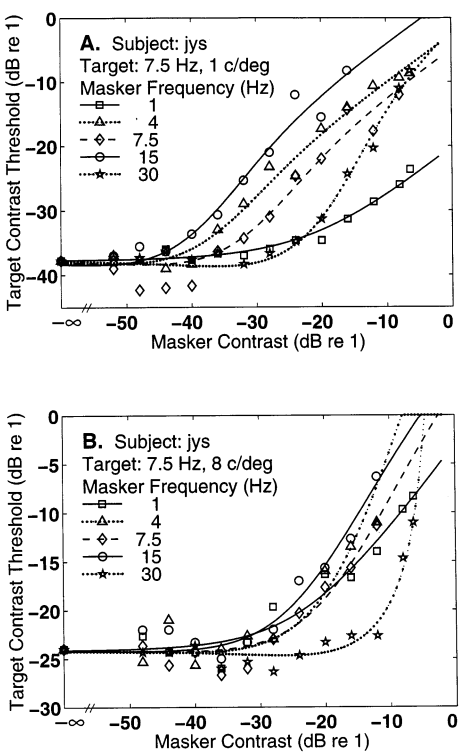

Fig. 8. Results of Experiment 2, subject JYS. All targets were 7.5 Hz, and target and masker spatial frequencies were 1 (A) or 8 (B) cpd.

Table 4
Slopes of regression line through the rising portion of TvC functions of Experiment 2

	GMB			JYS	
	1 cpd	5 cpd	8 cpd	1 cpd	8 cpd
1 Hz	0.84	0.56	0.64	0.64	0.61
4 Hz	0.86	0.72	0.94	0.84	0.75
7.5 Hz	0.81	0.79	1.14	0.91	0.97
15 Hz	0.94	0.67	0.92	1.10	0.82
30 Hz	1.06	0.54	1.16	1.54	1.26
Mean	0.902	0.656	0.960	1.006	0.882

excitatory tuning is very broad. The shape of the inhibitory tuning functions is broad and varies little across all three spatial frequencies. Inhibition is greatest for the 1 cpd conditions and for the 4–15 Hz temporal frequency range of the masker.

Table 5
Description of the model parameters

Parameter	Description
Nonlinear excitation model, one mechanism (NE_1)	
S_{Em}	Excitatory sensitivity to the masker
S_{Et}	Excitatory sensitivity to the target
p	Excitatory exponent
Z	Denominator parameter (fixed to 1.0)
Nonlinear excitation model, two mechanisms (NE_2)	
S_{Em1}	1st mechanism excitatory sensitivity to the masker
S_{Et1}	2nd mechanism excitatory sensitivity to the target
S_{Em2}	1st mechanism excitatory sensitivity to the masker
S_{Et2}	2nd mechanism excitatory sensitivity to the target
n	Nonlinear pooling constant (fixed to 4)
p	Excitatory exponent
Z	Denominator parameter (fixed to 1.0)
Divisive inhibition model (DI)	
S_{Em}	Excitatory sensitivity to the masker
S_{Im}	Inhibitory sensitivity to the masker
S_{Et}	Excitatory sensitivity to the target
S_I	Inhibitory sensitivity to the target
p	Excitatory exponent
q	Inhibitory exponent
Z	Denominator parameter (fixed to 1.0)

As in Experiment 1, excitatory and inhibitory sensitivity estimates are similar in magnitude when the masker temporal frequency is the same or similar to the target frequency (7.5 Hz). For the 1 and 5 cpd conditions, excitatory sensitivity drops below inhibitory sensitivity for the lowest frequency (1 Hz) masker. Thus at 1 and 5 cpd, excitatory tuning is narrower than inhibitory tuning. However, at 8 cpd excitatory and inhibitory sensitivities are nearly identical for all masker temporal frequencies.

5.3. Target sensitivities

The parameters S_{Et} and S_{It} (Tables 1 and 2) are excitatory and inhibitory sensitivity estimates of the detecting mechanism. In all cases, target excitatory sensitivity is greater than target inhibitory sensitivity. This differs from estimates of sensitivity to the masker, where inhibitory sensitivity is generally broader and greater than excitatory sensitivity. One possible explanation is that the inhibitory component, in addition to being broadly tuned to spatial and temporal frequencies, might also be sensitive to a greater spatial extent than the excitatory component. This would predict a greater sensitivity to the full-field masker than the restricted Gabor target. Foley (1994) found that a full-field masker masked more than a Gabor masker.

Excitatory and inhibitory target sensitivities estimated from Experiment 1 (2 cpd target) are greater than for the 10 Hz target and for the 1 Hz target. This is consistent with the masker excitatory and inhibitory sensitivities for all conditions except those with a target spatial frequency of 8 cpd.

6. Discussion

This study shows that TvC functions for different temporal frequency maskers differ greatly both in the magnitude of facilitation and in the slopes of the rising segments. This is a clear failure of the horizontal translation rule and is qualitatively inconsistent with the NE_1 and NE_2 models.

The NE models have survived until recently because they were not adequately tested. Although they successfully predict individual TvC functions, the models fail (both qualitatively and in goodness-of-fit) when tested with threshold measurements for a single target in the presence of maskers of differing masker temporal frequency and contrast. The NE_1 model predicts equal slopes of the rising segments of the TvC functions and constant facilitation. The multiple-mechanism version allows for different slopes, but also predicts constant facilitation. We found slopes to vary greatly within a family of TvC functions that share a single target. Also,

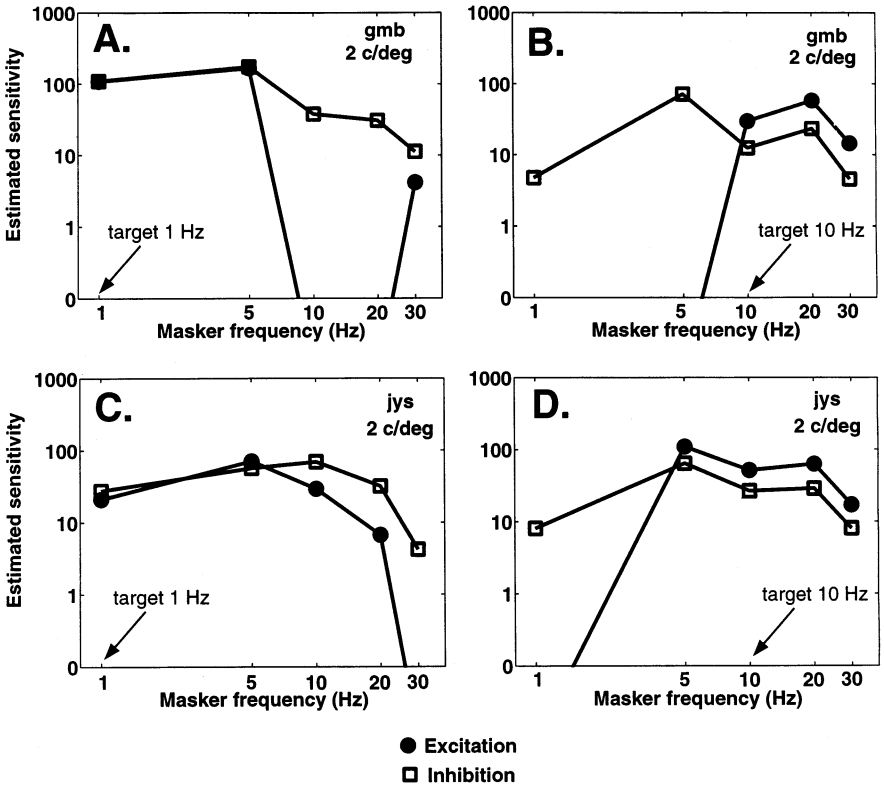

Fig. 9. Estimated mechanism sensitivity values from Experiment 1.

facilitation varied within each family of TvC functions, with maximal facilitation when target and masker were of the same temporal frequency. Such interactions between the contrast of the masker and other properties of the masker have been discovered previously for other classes of patterns (Georgeson & Georgeson, 1987; Ross & Speed, 1991; Foley & Boynton, 1994; Foley, 1994).

We have shown that across a wide variety of stimuli in the spatio-temporal domain that the DI model provides both a good fit and a statistically significant improvement in fit over the NE_1 model (with root mean error slightly larger than standard error). The DI model also fits better than the NE_2 model, even though the two models have the same number of free parameters. The DI model successfully describes the variation in the shapes of TvC functions across masker temporal frequency. It has previously been shown to describe TvC functions for different masker orientations relative to the target (Foley, 1994). Although the new model fits well, the best fit does not always capture the facilitation that occurs when target and masker temporal frequencies are equal. This failure is not well understood and merits more study.

The relation between masker temporal frequency and threshold elevation found here differs in one important way from results in the literature. Masking functions from Lehky (1985) and Hess and Snowden (1992) are concave down. In our experiments using 7.5 and 10 Hz targets, we found less masking when masker and target are of the same temporal frequency than when the masker frequency is just above or below the target frequency. This phenomenon was also found using target temporal frequencies of 5, 15 and 30 Hz (Boynton & Foley, 1991). We believe that this discrepancy can be explained by differences in experimental paradigms; unlike our study, both the Lehky (1985) and Hess and Snowden (1992) studies imposed a slight difference between target and masker. Lehky (1985) offset the orientation of the target, and Hess and Snowden (1992) randomly varied the temporal phase of the target with respect to the masker. Since facilitation is maximal when target and masker are similar (Legge & Foley, 1980; Georgeson, 1987), these changes minimize differences in facilitation effects across conditions.

Without these differences between the target and masker, facilitation occurs when target and masker have similar temporal frequencies. According to the DI model, the facilitation effect is the result of excitation by the masker. The facilitation effect lowers the entire rising portion of the TvC function. This explains why threshold elevation is not always maximal when the masker and target temporal frequencies are equal. The increased excitatory sensitivity to the masker shifts the TvC functions (when target and masker frequency are similar) downward for all masker contrasts (Fig. 2).

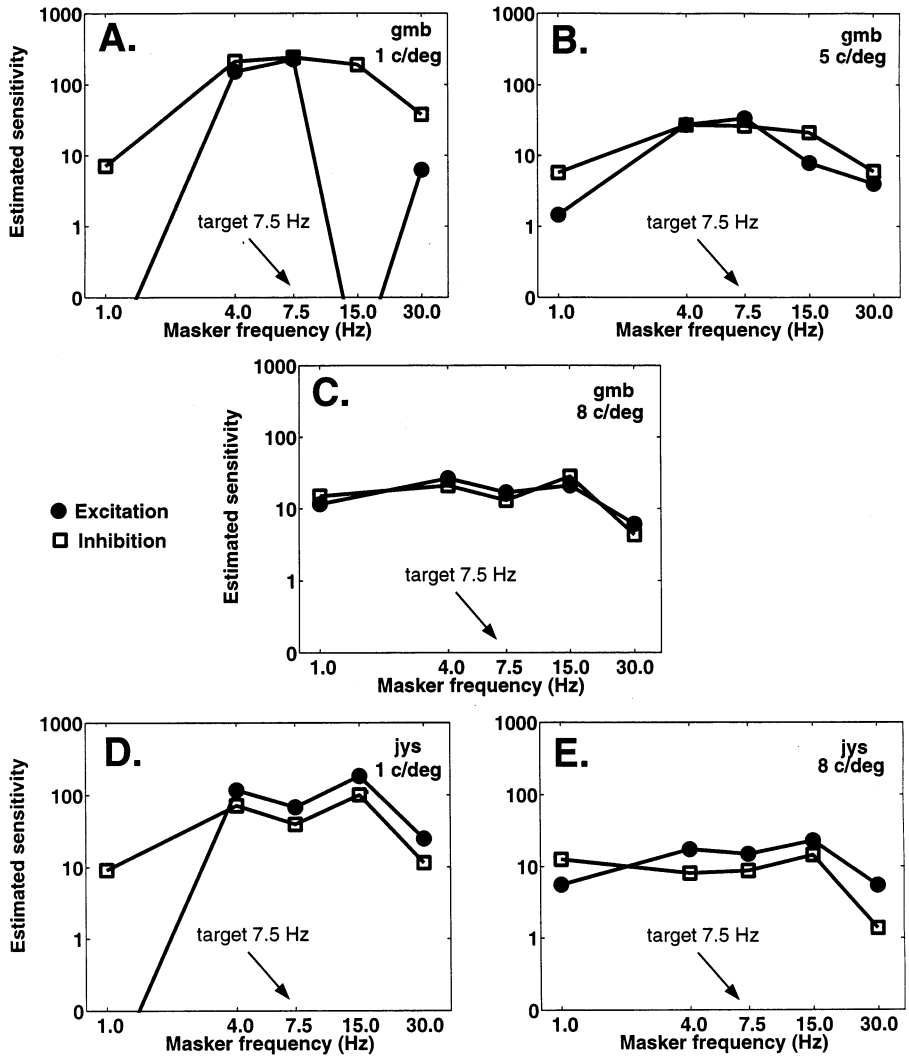

Fig. 10. Estimated mechanism sensitivity values from Experiment 2.

This study has two important implications for the interpretation of earlier masking studies. First, the variability in the shape of the TvC functions with masker frequency found in our study shows that the bandwidth of traditionally measured masking functions will vary with masker contrast. Thus, the masking functions measured by Hess and Snowden (1992) and Lehky (1985) do not generalize to maskers of all contrasts. Second, even if the variability in the shapes of TvC functions within a family are small, masking functions still do not directly reflect mechanism sensitivity functions, according to the DI model. The DI model predicts that the amount of masking at a single masker contrast is a consequence of both excitatory and inhibitory sensitivity to the masker. These two sensitivities are different functions of temporal frequency.

Using the DI model and the masking paradigm with a variety of masker orientations, Foley (1994) has shown that the detecting pattern vision mechanism has a narrowly tuned excitatory input and a broadly tuned inhibitory input in the orientation domain. Similarly, in this paper we have shown, by masking with a variety of temporal frequencies, that excitatory sensitivity is more narrowly tuned to temporal frequency than is inhibitory sensitivity. Excitatory sensitivity generally peaks at the temporal frequency of the target. Inhibitory sensitivity is very broadly tuned and varies little across the families of TvC functions. Unlike masking across orientation, the difference in tuning between excitation and inhibition is much less dramatic along the temporal frequency dimension and disappears at a high (8 c/deg) spatial frequency.

It is possible that the excitatory and inhibitory temporal sensitivity functions estimated here reflect the tuning of a subset of a finite number of detecting mechanisms in the spatio-temporal domain. However, attempts to fit multiple families of TvC functions with the same sensitivity parameters failed. This suggests that there are that there are at least several spatio-temporal mechanisms with different sensitivities. The simi-

ilarity of the inhibitory sensitivities to the masker across families of TvC functions is encouraging. It seems likely that the inhibitory sensitivities reflect the pooled responses of differently tuned mechanisms. These underlying mechanisms may be the same as those measured by the excitatory sensitivity estimates.

The DI model was adapted to the temporal domain by assuming that the thresholds depend on the mechanism response at one moment in time. Although this model accounts for our results well, it does not account for the effect of target duration (Legge, 1978; Watson, 1979) or for the effect of relative temporal phase in masking (Breitmeyer & Ganz, 1977).

It seems very likely that a more elaborate model that specifies the mechanism response as a function of time and provides for integration of the response over time will be necessary to account for these effects.

7. Conclusion

We have shown that when one temporally modulated pattern is masked by another, the form of the TvC function varies greatly with the temporal frequency of the patterns. These data are poorly fitted by a one-mechanism nonlinear excitation model. A two-mechanism nonlinear excitation model does not fit as well as a divisive inhibition model. Fits of the divisive inhibition model to the data indicate that a different mechanism detects each of the five target patterns. This indicates that there are several spatio-temporal pattern mechanisms in the human visual system that differ in their response functions as well as their tuning. These fits also suggest that excitatory tuning is narrower than divisive inhibitory tuning except at high spatial frequencies where they are approximately the same. Finally, excitatory tuning is low-pass for mechanisms tuned to low temporal frequencies and high spatial frequencies, and band-pass for mechanisms tuned to high temporal frequencies and low spatial frequencies.

Appendix A. Degrees of freedom in the divisive inhibition model

This Appendix discusses the free parameters of the DI model. The seven parameters consist of two excitatory sensitivities (one for the masker and one for the target) two inhibitory sensitivities, two exponents (p and q), and the constant Z. The mechanism response to a stimulus is:

$$R(E, I) = \frac{E^p}{I^q + Z} \tag{10}$$

If the parameter Z is changed by a scale factor to kZ, the values of E and I can be scaled so that the mechanism response stays the same because:

$$R(E, I) = \frac{E^p}{I^q + Z} = \frac{(k^{1/p}E)^p}{(k^{1/q}I)^p + kZ} \tag{11}$$

The equation above shows that scaling Z by a factor k can be offset by scaling E by $k^{1/p}$ and scaling I by $k^{1/q}$. Recall that the quantities E and I are products of stimulus contrast and mechanism sensitivities. Scaling Z can therefore be offset by scaling the excitatory and inhibitory sensitivities appropriately. Thus the seven parameters share only 6 d.f. For this reason Z was arbitrarily set to one for all model fits in this paper.

References

Albrecht, D. G., & Geisler, W. S. (1991). Motion sensitivity and the contrast-response funtion of simple cells in the visual cortex. *Visual Neuroscience*, *7*, 531–546.

Anderson, S. J., & Burr, D. C. (1985). Spatial and temporal selectivity of the human motion detection system. *Vision Research*, *25*, 1147–1154.

Boynton, G. M., & Foley, J. M. (1991). Adapting to temporally modulated spatial patterns: effects of temporal frequency and adapter contrast. *Association for Research in Vision and Ophthalmology*, *32*, 851.

Breitmeyer, B. G. (1975). Simple reaction time as a measure of the temporal response properties of transient and sustained channels. *Vision Research*, *15*, 1411–1412.

Breitmeyer, B., & Ganz, L. (1977). Temporal studies with flashed gratings: inferences about human transient and sustained channels. *Vision Research*, *17*, 861–865.

Burbeck, C., & Kelly, D. (1980). Spatiotemporal characteristics of visual mechanisms: excitatory-inhibitory model. *Journal of the Optical Society of America A*, *70*, 1121–1126.

Campbell, F. W., & Robson, J. G. (1967). Application of Fourier analysis to the visibility of gratings. *Journal of Physiology* (*London*), *197*, 551–556.

Foley, J. M. (1994). Human luminance pattern-vision mechanisms: masking experiments require a new model. *Journal of the Optical Society of America A*, *11*, 1710–1719.

Foley, J. M., Boynton, G. M. (1994). A new model of human luminance pattern vision mechanisms: analysis of the effects of pattern orientation, spatial phase, and temporal frequency. In: T. A., Lawton, *Computational vision based on neurobiology*, *SPIE Proceedings*, vol. 2054.

Georgeson, M. A. (1987). Temporal properties of spatial contrast vision. *Vision Research*, *27*, 765–780.

Gerogeson, M., & Georgeson, J. (1987). Facilitation and masking of briefly presented gratings: time-course and contrast dependence. *Vision Research*, *27*, 369–379.

Green, M. (1981). Psychophysical relationships among mechanisms sensitive to pattern, motion and flicker. *Vision Research*, *21*, 971–983.

Harwerth, R. S., & Levi, D. M. (1978). Reaction time as a measure of suprathreshold grating detection. *Vision Research*, *18*, 1579–1586.

Heeger, D. J. (1992). Normalization of cell responses in cat striate cortex. *Visual Neuroscience*, *9*, 181–198.

Hess, R., & Plant, G. (1985). Temporal frequency discrimination in human vision: evidence for an additional mechanism in the low spatial and high temporal frequency region. *Vision Research*, *25*, 1493–1500.

Hess, R., & Snowden, R. (1992). Temporal properties of human visual filters: number, shapes and spatial covariation. *Vision Research*, *32*, 47–59.

Keesey, U. T. (1972). Flicker and pattern detection: a comprison of thresholds. *Journal of the Optical Society of America*, *62*, 444–448.

Kelly, D. (1972). Flicker. In Hurvich, & Jameson, *Handbook of Sensory Physiology*. New York: Springer-Verlag.

Khuri, A., & Cornell, J. (1987). *Response surfaces*: *designs and analysis*. New York: Marcel Dekker.

King-Smith, P. E., & Kulikowski, J. J. (1975). Pattern and flicker detection analysed by subthreshold summation. *Journal of Physiology*, *249*, 519–548.

Koenderink, J. J., & van Doorn, A. J. (1979). Spatiotemporal contrast detection threshold suface is bimodal. *Optics Letters*, *4*, 845–849.

Kulikowski, J. J., & Tolhurst, D. J. (1993). Psychophysical evidence for sustained and transient detectors in human vision. *Journal of Physiology* (*London*), *232*, 149–162.

Legge, G. E. (1978). Sustained and transient mechanisms in human vision: temporal and spatial properties. *Vision Research*, *18*, 69–81.

Legge, G., & Foley, J. (1980). Contrast masking in human vision. *Journal of the Optical Society of America A*, *70*, 1458–1470.

Lehky, S. (1985). Temporal properties of visual channels measured by masking. *Journal of the Optical Society of America A*, *2*, 1260–1272.

Mandler, M. (1984). Temporal frequency discriminations above threshold. *Vision Research*, *12*, 1873–1880.

Mandler, M., & Makous, W. (1984). A three channel model of temporal frequency perception. *Vision Research*, *24*, 1881–1887.

Pantle, A. (1983). Temporal determinants of spatial sine-wave masking. *Vision Research*, *23*, 749–757.

Press, W. H., Flannery, B. P., Teulolsky, S. A., & Vetterling, W. T. (1998). *Numerical recipes in C*. Cambridge: Cambridge University Press.

Richards, W. (1979). Quantifying sensory channels: Generalizing colorimetry to orientation and texture, touch and tones. *Sensory Processes*, *3*, 207–229.

Robson, J. G. (1966). Spatial and temporal contrast sensitivity functions of the visual system. *Journal of the Optical Society of America*, *56*, 1141–1142.

Ross, J., & Speed, H. D. (1991). Contrast adaptaion and contrast masking in human vision. *Proceedings of the Royal Society of London*, *B*, *246*, 61–69.

Stiles, W. S. (1949). Increment thresholds and the mechanisms of colour vision. *Documenta Opthalmologica*, *3*, 138–163.

Tartaglione, A., Goff, D. P., & Benton, A. L. (1975). Reaction time to square-wave gratings as a function of spatial frequency, complexity and contrast. *Brain Research*, *100*, 111–120.

Teo, P., & Heeger, D.J. (1994). Perceptual image distortion, *Proceedings of SPIE*, vol. 2179, San Jose, CA, pp. 127–141.

Thompson, P. G. (1983). Discrimination of moving gratings at and above detection threshold. *Vision Research*, *23*, 1533–1538.

Tolhurst, D. J. (1975). Sustained and transient channels in human vision. *Vision Research*, *15*, 1151–1155.

van Nes, F. L., Koenderink, J. J., Nas, H., & Bouman, M. (1967). Spatio-temporal modulation transfer in the human eye. *Journal of the Optical Society of America*, *57*, 1082–1088.

Watson, A. (1979). Probability summation over time. *Vision Research*, *19*, 515–522.

Watson, A. B. (1986). Temporal sensitivity. In K. R. Boff, L. Kauffman, & J. P. Thomas, *Handbook of perception and human performance*. In: *Sensory processes and perception*, Vol. 1. New York: Wiley.

Watson, A., & Robson, J. (1981). Discrimiation at threshold: Labelled detectors in human vision. *Vision Research*, *21*, 1115–1122.

Watson, A., & Pelli, D. (1983). Quest: A bayesian adaptive psychometric method. *Perception and Psychophysics*, *33*, 113–120.

Watson, A. B., & Soloman, J. A. (1997). Model of visual contrast gain control and pattern masking. *Journal of Optical Society of America A*, *14*, 2379–2391.

Watson, A. B., Nielson, K. R. K., Poirson, A., Fitzhugh, A., Bilson, A., Nguyen, K., & Nguyen, A. J. A. Jr. (1986). Use of a raster framebuffer in vision research. *Behavior Research Methods and Instrumentation Computers*, *18*, 587–594.

Wilson, H., McFarlane, D., & Phillips, G. (1983). Spatial frequency tuning of orientation sensitive units estimated by oblique masking. *Vision Research*, *23*, 872–882.